Vibrational spectroscopy favors a unique QB binding site at the proximal position in wild-type reaction centers and in the Pro-L209 --> Tyr mutant from Rhodobacter sphaeroides.

ARTICLE *in* BIOCHEMISTRY · OCTOBER 2002

Impact Factor: 3.02 · Source: PubMed

6 AUTHORS, INCLUDING:

Pierre Sebban
Université Paris-Sud 11
77 PUBLICATIONS **1,525** CITATIONS
SEE PROFILE

Laura Baciou
French National Centre for Scientific Research
44 PUBLICATIONS **889** CITATIONS
SEE PROFILE

Vibrational Spectroscopy Favors a Unique Q_B Binding Site at the Proximal Position in Wild-Type Reaction Centers and in the Pro-L209 → Tyr Mutant from *Rhodobacter sphaeroides*

Jacques Breton,[‡] Claude Boullais,[§,||] Charles Mioskowski,[§] Pierre Sebban,[⊥] Laura Baciou,[⊥] and Eliane Nabedryk*[,‡]

Service de Bioénergétique and Service de Marquage Moléculaire et de Chimie Bioorganique, CEA-Saclay, 91191 Gif-sur-Yvette, France, and Centre de Génétique Moléculaire, CNRS, 91198 Gif-sur-Yvette, France

Received August 2, 2002; Revised Manuscript Received September 19, 2002

ABSTRACT: In the various X-ray structures of native reaction centers (RCs) from the photosynthetic bacterium *Rhodobacter sphaeroides*, two distinct main binding sites (distal and proximal) for the secondary quinone Q_B have been described in the literature. The movement of Q_B from its distal to proximal position has been proposed to account for the conformational gate limiting the rate of the first electron transfer from the primary quinone Q_A^- to Q_B. Recently, Q_B was found to bind in the proximal binding site in the dark-adapted crystals of a mutant RC where Pro-L209 was changed to Tyr [Kuglstatter, A., Ermler, U., Michel, H., Baciou, L., and Fritzsch, G. (2001) *Biochemistry 40*, 4253−4260]. To test the structural and functional implications of the distal and proximal sites, a comparison of the FTIR vibrational properties of Q_B in native RCs and in the Pro-L209 → Tyr mutant was performed. Light-induced FTIR absorption changes associated with the reduction of Q_B in Pro-L209 → Tyr RCs reconstituted with ^{13}C-labeled ubiquinone (Q_3) at the 1 or 4 position show a highly specific IR fingerprint for the C═O and C═C modes of Q_B upon selective labeling at C_1 or C_4. This IR fingerprint is very similar to that of native RCs, demonstrating that equivalent interactions occur between neutral Q_B and the protein in native and mutant RCs. Consequently, Q_B occupies the same binding site in all RCs. Since the FTIR data fit the description of Q_B bonding interactions in the proximal site, it is therefore concluded that neutral Q_B also binds to the proximal site in native functional RCs. The implication of these new results for the conformational gate of the first electron transfer to Q_B is outlined.

The reaction center (RC)[1] from photosynthetic purple bacteria is a membrane-bound pigment-protein complex that uses light energy to couple sequentially the transfer of two electrons and two protons to the secondary quinone Q_B, leading to the formation of the quinol species which then diffuses out the RC to be replaced with an oxidized quinone of the pool (*1*). In contrast to the mobile Q_B which functions as a two-electron gate, the tightly bound primary quinone Q_A is a one-electron acceptor that is never protonated. The X-ray structures of the two most thoroughly investigated bacterial RCs, i.e., those from *Rhodobacter* (*Rb.*) *sphaeroides* and *Rhodopseudomonas* (*Rp.*) *viridis* (for a review, see ref *2*), revealed different properties of the binding pockets for Q_A and Q_B. The environment of Q_B is much more polar than the Q_A site. Moreover, while the binding of Q_A is well-defined, different locations of Q_B have been observed in the various crystallographic structures reported for both RCs, and two distinct main binding sites for Q_B have been discussed. Early X-ray structures of RCs from *Rb. sphaeroides* (*3*−*6*) and *Rp. viridis* (*7*−*9*) show Q_B with a position proximal to the non-heme iron (closest to Q_A), with possible hydrogen bonds at both carbonyls. However, in these early structures, the Q_B site was often poorly defined due to the low occupancy of Q_B. Ermler et al. (*10*) were the first to describe a different position of Q_B in the RC from *Rb. sphaeroides* (at 2.65 Å resolution; PDB entry 1PCR) with Q_B displaced by ∼5 Å and occupying a position termed the distal site (furthest from the non-heme iron) with only one carbonyl hydrogen bonded to the protein; however, in this distal site, Q_B was presumed to be in the ubiquinol (Q_BH_2) state. A major finding was reported by Stowell et al. (*11*) when they obtained, at cryogenic temperature, the dark-adapted (PDB entry 1AIJ) and light-adapted (PDB entry 1AIG) structures (at 2.2 and 2.6 Å resolution, respectively) for *Rb. sphaeroides* RCs containing a mixture of native Q_B (Q_{10}) and added Q_2, with quantitative occupancy (60−70%) of the Q_B site. In the dark-adapted state, Q_B was mainly found in the distal position with the O_4 carbonyl oxygen hydrogen bonded to the polypeptide backbone (Ile-L224). In the charge-separated state ($P^+Q_B^-$) of *Rb. sphaeroides* RCs at 90 K, Q_B^- has moved by ∼4.5 Å and has undergone a 180°

* To whom correspondence should be addressed: SBE, CEA-Saclay, Bât. 532, 91191 Gif-sur-Yvette CEDEX, France. Phone: 331 69 08 71 12. Fax: 331 69 08 87 17. E-mail: nabedryk@dsvidf.cea.fr.

‡ Service de Bioénergétique, CEA-Saclay.

§ Service de Marquage Moléculaire et de Chimie Bioorganique, CEA-Saclay.

|| Current address: DCS, CEA Fontenay-aux-Roses, Bât. 19, BP 6, 92265 Fontenay-aux-Roses CEDEX, France.

⊥ Centre de Génétique Moléculaire CNRS.

[1] Abbreviations: RC, reaction center; Q_A and Q_B, primary and secondary quinone electron acceptors, respectively; Q_n, 2,3-dimethoxy-5-methyl-6-polyprenyl-1,4-benzoquinone; P, primary electron donor; FTIR, Fourier transform infrared spectroscopy.

10.1021/bi026565k CCC: $22.00
Published on Web 00/00/0000 PAGE EST: 6.7

flip of the quinone ring around the isoprenoid chain; Q_B^- now occupies a proximal position with both carbonyls hydrogen bonded to the protein (notably to His-L190). Reinvestigation of the original data set (*8*) for *Rp. viridis* RCs (PDB entry 1PRC) has led to a new model (PDB entry $1PRC_{new}$) for native Q_B (Q_9) with occupancies of 30 and 20% of the distal and proximal sites, respectively (*12*−*14*). However, the structurally best described Q_B site in *Rp. viridis* RCs was obtained (at 2.45 Å resolution) for RCs reconstituted with Q_2 (PDB entry 2PRC) where the quinone has a well-defined proximal position with full occupancy of the Q_B site (*12*).

The difference between the "light" and "dark" structures has offered a molecular basis for a model of the electron transfer from the primary quinone to Q_B. The proximal site for Q_B was postulated to be an activated site for electron transfer, while the distal site was assumed to be inactive in electron transfer (*11*). The movement of Q_B from its distal to proximal site was proposed to account for a conformational gate limiting the rate of the first electron transfer from $Q_A^-Q_B$ to $Q_AQ_B^-$ (*12*, *15*). Lancaster and Michel (*12*) had already proposed a mechanistic model for intermediates in the reaction cycle of quinone reduction to ubiquinol in *Rp. viridis* RCs. This model involves different binding sites for Q_B, Q_B^-, Q_BH^-, and Q_BH_2. In the past two years, the conformational gating mechanism has triggered a number of theoretical works on the functional implications of the two distinct binding sites of Q_B. Calculations on the energetics of the electron transfer from Q_A^- to Q_B in *Rb. sphaeroides* RCs have indicated that electron transfer is more favorable when Q_B is in the proximal site (*16*). Molecular dynamics simulations of Q_B binding in the RC of *Rb. sphaeroides* (*17*) and *Rp. viridis* (*14*) support the spontaneous transfer of Q_B from the distal site to the proximal site, notably when the primary quinone Q_A becomes reduced (*14*). The existence of two binding sites has been proposed to be related to different protonation states of the two nearby amino acids, Glu-L212 and Asp-L213 (*16*, *17*), that are important for rapid electron-coupled proton transfer to reduced Q_B (*1*, *18*). A mechanistic model of the Q_B turnover in *Rb. sphaeroides* RCs also assumed two possible configurations of the quinone, depending on the equilibrium between the ionized and protonated forms of Glu-L212 (*19*). Very recently, the orientation of the Glu-L212 side chain was described as the possible conformational gate for the Q_B migration which may control the first electron transfer (*20*). Although the distal to proximal change of position of the quinone has been given important functional relevance for the gating process of the Q_A^- to Q_B electron transfer, it should be recognized that the redox state of Q_B in both the distal and proximal sites of the crystallographic structures is still uncertain.

Very recently, Q_B was found to bind essentially in the proximal position in the crystallographic structures resolved near room temperature of several mutant RCs from *Rb. sphaeroides*[2] near the quinone sites. The mutation of Ala-M260 to Trp (PDB entry 1QOV) leads to the absence of Q_A in the protein complex, resulting in an RC in which the electron transfer to Q_A, and thus to Q_B, is abolished (*21*, *22*). In the double mutant Glu-L212 → Ala/Asp-L213 → Ala [PDB entry 1K6N (*23*)], the transfer of the first proton to reduced Q_B is interrupted and Q_B^- is extremely stable (*24*). On the other hand, in the Pro-L209 → Tyr mutant RC which was originally constructed to interrupt a water chain in the RC protein (*10*, *25*), the first electron transfer to Q_B is not significantly changed, while the second electron transfer and the proton uptake rates are decreased by ∼2−3-fold compared to those of native RCs (*25*−*27*). These characteristics make the Tyr-L209 RCs amenable to vibrational spectroscopic investigations of Q_B and Q_B^- in an RC which shows Q_B in the proximal site in dark-adapted RC crystals at 5 °C [PDB entry 1F6N (*28*)].

Other than studies involving the crystallographic determination of the positions of Q_B in RCs, experimental approaches to testing the structural characteristics of the distal and proximal positions are scarce. Light-induced FTIR difference spectroscopy has proven its ability to explore the structural and functional properties of the Q_A and Q_B sites in wild-type RCs from *Rb. sphaeroides* and *Rp. viridis* (*29*−*37*) as well as in mutant RCs (*38*−*45*). In particular, FTIR studies of *Rb. sphaeroides* and *Rp. viridis* RCs reconstituted with site-specific isotope-labeled quinones have provided precise information about the bonding interactions of Q_A (*31*, *32*, *36*) and Q_B (*33*−*35*, *45*) with the surrounding protein. On one hand, these studies have demonstrated greatly different vibrational IR patterns for the Q_A and Q_B binding sites in *Rb. sphaeroides* RCs (*31*−*35*) and, on the other hand, similar IR patterns for the interactions of the quinone with the protein at the Q_B site in both *Rb. sphaeroides* and *Rp. viridis* RCs (*33*). Although Q_A and Q_B are identical molecules (Q_{10}) in native *Rb. sphaeroides* RCs, a large asymmetry between the two carbonyls of Q_A has been revealed by FTIR difference spectroscopy, while the interactions of the two carbonyls of Q_B with the protein binding site are equivalent. Thus, the same molecule of ubiquinone either in the Q_A or in the Q_B binding site (*31*, *33*) displays completely different IR signatures that are also very distinct from those of the quinone in vitro (*31*, *33*, *46*, *47*). Moreover, it should be emphasized that a control of the functionality of the quinone at the Q_B site can be performed under the conditions of the FTIR experiments by measuring the characteristic oscillation pattern with a period of 2 when the quinone evolves between the Q_B, Q_B^-, and Q_BH_2 states upon excitation of RCs with a sequence of flashes (*48*, *49*). Notably, it has been demonstrated that upon sequential flash excitation of RCs, the shape of the light-induced FTIR difference spectra exhibits a clear fingerprint for Q_B^- formation on odd-numbered flashes and distinct features on even-numbered flashes (*30*). Although the one-electron reduction of the secondary quinone has been monitored in RC crystals (*11*, *50*), the oscillatory behavior of the formation and destruction of the semiquinone state on a sequence of successive flashes has, however, not been reported so far for the secondary quinone in RCs crystals. Another advantage of using FTIR spectroscopy is that IR samples do not contain additives such as crystallizing agents when making crystals or cryoprotectants when freezing the sample for optical studies (*27*).

With respect to the question under debate, i.e., the functional relevance of the two distinct main sites of Q_B in native RCs, the isotopic effects on the Q_B^-/Q_B FTIR

[2] In the structural model of the His-L168 → Phe mutant RC from *Rb. sphaeroides* (*58*), the conformation adopted by Q_B is also the proximal one, although the mutation occurs close to one of the two bacteriochlorophylls that constitutes P.

difference spectra of *Rb. sphaeroides* and *Rp. viridis* RCs easily fit the description of symmetric hydrogen bonding interactions at both carbonyls occurring in the proximal position (*11*, *12*). However, as pointed out in refs *11* and *12*, these effects are more difficult to reconcile with the bonding interactions proposed at the distal site, i.e., with a single hydrogen bond between the distal carbonyl of Q_B and the polypeptide backbone. While the FTIR analysis of RCs cannot directly distinguish between Q_B in the proximal or distal conformation, the specificity of the method allows very precise differences in the bonding interactions of a quinone in different environments to be detected. Such an approach should be well-suited to investigating mutant RCs where Q_B occupies the proximal site, even in the dark-adapted RC crystals.

In the work presented here, the effects of substituting Pro-L209 with Tyr in RCs from *Rb. sphaeroides* are investigated by monitoring the light-induced FTIR absorption changes associated with the photoreduction of Q_B. The Tyr-L209 mutant RCs were reconstituted with site-specific ^{13}C-labeled ubiquinone to determine the bonding interactions of Q_B. A comparison of the FTIR results obtained on Tyr-L209 RCs with those previously reported for wild-type RCs from *Rb. sphaeroides* (*33*−*35*) and *Rp. viridis* (*33*) allows the functional implications of the distal and proximal Q_B sites to be reexamined.

EXPERIMENTAL PROCEDURES

The construction of the Pro-L209 → Tyr site-directed mutant and the isolation of purified RCs are described in ref *25*. A detailed description of the preparation of RC samples for FTIR experiments is given in refs *38* and *40*. RC samples in 90 mM Tris buffer (pH 7) contained an excess of ubiquinone (Q_6 or Q_3). Q_6 was purchased from Sigma. The synthesis of Q_3 selectively labeled with ^{13}C at the 1 or 4 position has been reported previously (*47*).

Steady-state light-induced FTIR difference spectra of the Q_B to Q_B^- transition in native and mutant RCs were recorded at 15 °C with a Nicolet 60SX spectrometer, as described in refs *33* and *38*. The Q_B^- state was generated by excitation with a single saturating flash (Nd:YAG laser, 7 ns, 530 nm). Difference spectra were calculated from each of 128 scans (acquisition time of 23 s) recorded before and after laser flash excitation. For a given sample, these measurements were repeated over ∼30 h. Spectra are an average of two to three samples.

RESULTS AND DISCUSSION

Comparison of Q_B^-/Q_B FTIR Spectra of Wild-Type RCs and of the Pro-L209 → Tyr Mutant. Figure 1 shows the Q_B^-/Q_B light-induced FTIR difference spectra of wild-type and Tyr-L209 mutant RCs reconstituted with unlabeled Q_6. In wild-type RCs (Figure 1b), absorption changes associated with the first electron transfer to Q_B have been previously correlated with modes of the semiquinone (C⋯O and C⋯C at 1479 cm^{-1}), the neutral quinone (C═O at 1641 cm^{-1}, C═C at 1617 cm^{-1}, C−O−CH_3 at 1265 and 1290 cm^{-1}), and the protein (*33*). The protein modes include the C═O stretching at 1728 cm^{-1} of the Glu-L212 protonated side chain (*38*, *39*), the amide I (80% peptide C═O stretching) at 1685, 1651, and 1641 cm^{-1}, and the amide II (60% peptide NH bending and 40% CN stretching) at 1537 and 1527 cm^{-1}.

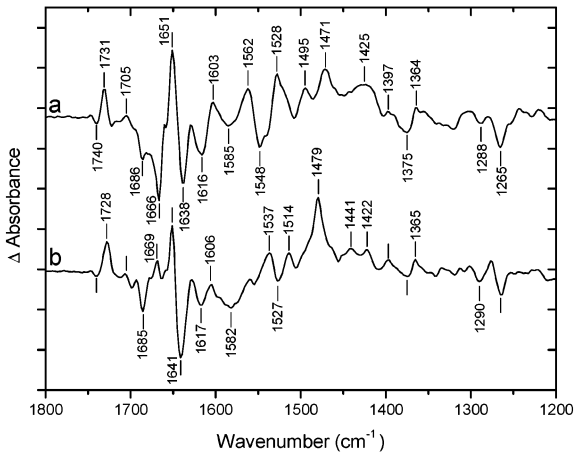

FIGURE 1: Light-induced Q_B^-/Q_B FTIR difference spectra of Pro-L209 → Tyr mutant (a) and wild-type (b) RCs from *Rb. sphaeroides* reconstituted with unlabeled Q_6 at pH 7 and 15 °C. Approximately 100 000 interferograms were averaged. Each division on the vertical scale corresponds to 2×10^{-4} absorbance unit. The frequency of the IR bands is given with an accuracy of ±1 cm^{-1}. The spectral resolution was 4 cm^{-1}.

The Q_B^-/Q_B spectrum of the Tyr-L209 mutant RC (Figure 1a) displays drastic changes compared to that of native RCs, notably in the protein absorption range (at 1666, 1562, 1548, and 1528 cm^{-1}) and between 1500 and 1400 cm^{-1}. Instead of the main semiquinone band seen at 1479 cm^{-1} in native RCs, the spectrum of the mutant shows two bands at 1471 and 1495 cm^{-1}. Such FTIR changes can be related either to different responses of the protein upon semiquinone formation in native and mutant RCs or to the different position of the quinone in the mutant (*28*). Identification of the IR fingerprint of Q_B for the Tyr-L209 mutant using RCs reconstituted with isotopically labeled ubiquinone is thus required for an unambiguous attribution of the Q_B and Q_B^- modes with respect to those of the protein.

Q_B and Q_B^- IR Fingerprints of the Pro-L209 → Tyr Mutant: Study of RCs Reconstituted with Site-Specific ^{13}C-Labeled Ubiquinone. Interactions of Q_B and Q_B^- with the protein in the Tyr-L209 mutant RCs were investigated by using specifically labeled quinones to reconstitute the Q_B site. Spectra a−c of Figure 2 correspond to Q_B^-/Q_B spectra of RCs reconstituted with unlabeled Q_3, $^{13}C_1$-labeled Q_3, and $^{13}C_4$-labeled Q_3, respectively. In these spectra (Figure 2a−c), several regions, i.e., between 1750 and 1650 cm^{-1}, 1600 and 1500 cm^{-1}, and 1400 and 1200 cm^{-1}, appear to be unaffected by the quinone labeling; these features arise mostly from protein and unlabeled quinone (methyl, methoxy, and isoprenoid chain) modes. However, distinct isotopic effects for $^{13}C_1$ and $^{13}C_4$ labeling occur in the 1600−1625 cm^{-1} range and between 1500 and 1400 cm^{-1}. More specifically, a large single negative peak is present at 1618 cm^{-1} for $^{13}C_4$ labeling (Figure 2c), while two negative bands are observed at 1622 and 1600 cm^{-1} for $^{13}C_1$ labeling (Figure 2b). In the semiquinone absorption region, large amplitude increases of bands occur at 1493, 1438, and 1414 cm^{-1} upon labeling with $^{13}C_1$, and at 1444 and 1419 cm^{-1} upon labeling with $^{13}C_4$.

All these effects are best visualized in the "double-difference" spectra (Figure 2d,e) calculated from the individual Q_B^-/Q_B spectra recorded with RCs reconstituted with isotopically labeled and unlabeled Q_3 (^{13}C-minus-^{12}C). In

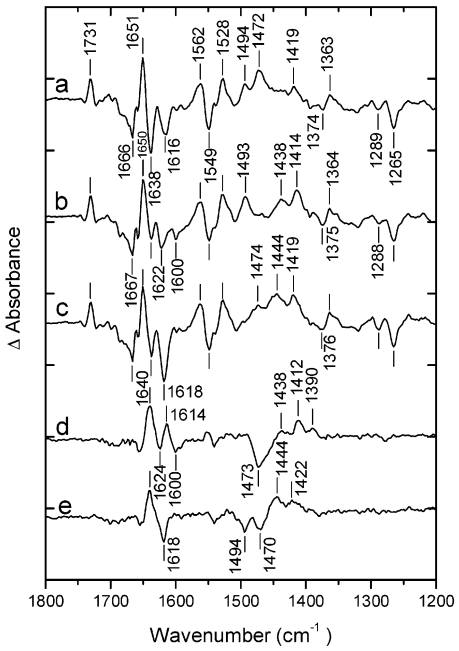

FIGURE 2: Light-induced Q_B^-/Q_B FTIR difference spectra at pH 7 and 15 °C of Pro-L209 → Tyr mutant RCs reconstituted with (a) unlabeled Q_3, (b) $^{13}C_1$-labeled Q_3, and (c) $^{13}C_4$-labeled Q_3. Calculated double-difference spectra (isotopically labeled-minus-unlabeled) obtained for $^{13}C_1$ labeling (d) and $^{13}C_4$ labeling (e). Approximately 70 000 interferograms were averaged. Each division on the vertical scale corresponds to 5×10^{-4} absorbance unit.

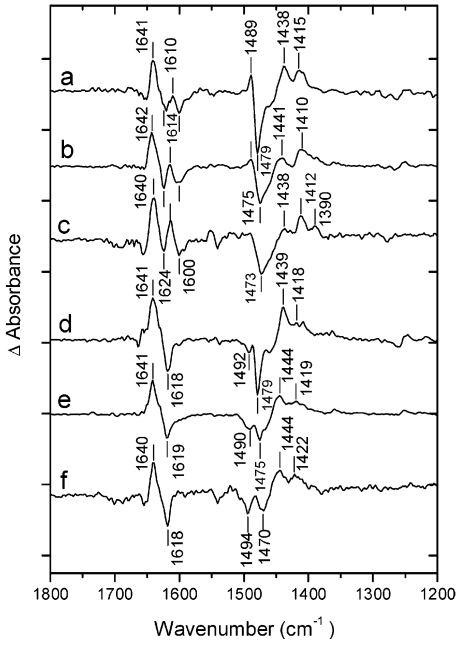

FIGURE 3: Calculated double-difference spectra (isotopically labeled-minus-unlabeled) obtained for RCs reconstituted with $^{13}C_1$-labeled Q_3 [(a) *Rb. sphaeroides*, (b) *Rp. viridis*, and (c) Pro-L209 → Tyr mutant] and $^{13}C_4$-labeled Q_3 [(d) *Rb. sphaeroides*, (e) *Rp. viridis*, and (f) Pro-L209 → Tyr mutant]. Each division on the vertical scale corresponds to 4×10^{-4} absorbance unit. Data for *Rb. sphaeroides* and *Rp. viridis* were taken from Breton et al. (*33*).

such double-difference spectra, isotope-sensitive vibrations from the quinone itself can be separated from those of the protein that are expected to cancel.[3] The double-difference spectra for $^{13}C_1$ ($^{13}C_1$-minus-^{12}C) and $^{13}C_4$ ($^{13}C_4$-minus-^{12}C) labeling are displayed as spectra d and e of Figure 2, respectively. In these spectra, the IR bands of the neutral unlabeled quinone (1660−1600 cm^{-1}) appear with a positive sign while the downshifted bands of the labeled quinone exhibit a negative sign. The semiquinone bands in the 1500−1400 cm^{-1} range exhibit a reverse behavior. Such double-difference spectra for $^{13}C_1$ and $^{13}C_4$ labeling represent fingerprints for the interactions of the quinone and semiquinone in their respective protein binding site (*33*). A detailed discussion of the semiquinone−protein interactions and of the response of the protein in the Tyr-L209 mutant will be given elsewhere. Briefly, the pattern of the bands corresponding to the unlabeled semiquinone (Figure 2d,e) shows one main negative band at 1473 cm^{-1} for $^{13}C_1$ labeling and two negative bands of comparable amplitude at 1494 and 1470 cm^{-1} for $^{13}C_4$ labeling. The pattern of the bands is also different for the labeled semiquinone (at 1438, 1412, and 1390 cm^{-1} for $^{13}C_1$ labeling and at 1444 and 1422 cm^{-1} for $^{13}C_4$ labeling).

As previously observed for wild-type RCs (*33*, *34*), an inequivalence of the C═C modes of neutral Q_B involving the C_1 and C_4 atoms is deduced from the observation of a differential signal at 1614/1600 cm^{-1} upon $^{13}C_1$ labeling while no such signal is present upon $^{13}C_4$ labeling. On the other hand, both double-difference spectra (Figure 2d,e) show a positive band at 1640 cm^{-1} which is downshifted to 1618 cm^{-1} upon $^{13}C_4$ labeling and to ∼1624 cm^{-1} upon $^{13}C_1$ labeling. The 1640 cm^{-1} band is attributed to the C═O vibrations of the unlabeled Q_B in the Tyr-L209 RCs. It therefore appears that both carbonyls of neutral Q_B absorb at the same frequency in the Tyr-L209 mutant RCs.

Comparison of the Q_B and Q_B^- IR Fingerprints in Wild-Type RCs from Rb. sphaeroides and Rp. viridis and in the Pro-L209 → Tyr Mutant. Figure 3 compares the $^{13}C_1$-minus-^{12}C (Figure 3a−c) and $^{13}C_4$-minus-^{12}C (Figure 3d−f) double-difference spectra of the three RCs (*Rb. sphaeroides*, *Rp. viridis*, and the Tyr-L209 mutant) reconstituted with the same quinones ([^{12}C]Q_3, [$^{13}C_1$]Q_3, and [$^{13}C_4$]Q_3). It is striking that the double-difference spectra of the Tyr-L209 mutant RC are very comparable to the ones previously obtained for wild-type *Rb. sphaeroides* and *Rp. viridis* RCs (*33*), notably with closely related IR patterns of bands in the 1650−1600 cm^{-1} (C═O and C═C) range that are specific for labeling at C_1 and C_4. The same IR pattern for the C═O and C═C modes of Q_B has also been observed in two other mutant RCs from *Rb. sphaeroides* reconstituted with [$^{13}C_1$]Q_3 and [$^{13}C_4$]Q_3: the single mutant Ser-L223 → Ala (*45*) and the double mutant Asp-L213 → Asn/Asn-M44 → Asp (E. Nabedryk, M. L. Paddock, M. Y. Okamura, and J. Breton, unpublished data).

In the carbonyl absorption range, all the spectra (Figure 3) display a positive band at 1641 ± 1 cm^{-1} which is identically downshifted to 1618−1619 cm^{-1} upon $^{13}C_4$ labeling, and to 1620−1624 cm^{-1} upon $^{13}C_1$ labeling. These data show that, in all the RCs, both C═O groups of Q_B contribute equally at 1641 ± 1 cm^{-1}. The isotopic shifts observed upon $^{13}C_1$ or $^{13}C_4$ labeling of the quinone for the 1641 cm^{-1} band (20 ± 3 cm^{-1}) are smaller than the shift

[3] In spectra d and e of Figure 2, the cancellation of the bands in the 1550 cm^{-1} spectral range and at ∼1655 cm^{-1} is not complete, leading to small signals attributed to residual amide I and amide II protein bands (also visible in spectra a and d of Figure 3). The signal-to-noise ratio of the spectra would have to be strongly increased to avoid such an apparent unperfect cancellation.

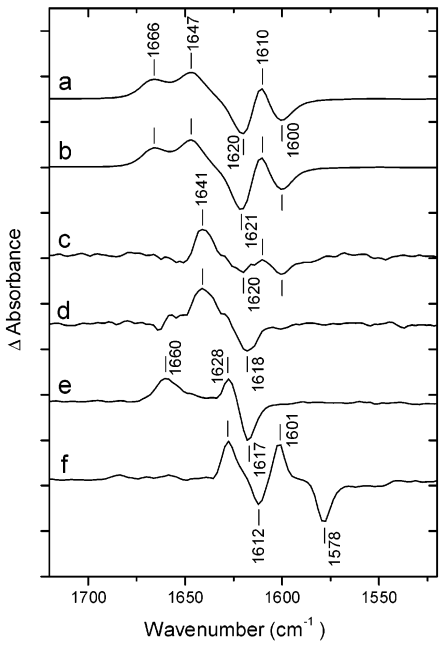

FIGURE 4: Calculated difference spectra between IR absorption spectra of films of unlabeled Q_3 and (a) $^{13}C_1$-labeled Q_3 and (b) $^{13}C_4$-labeled Q_3. Calculated double-difference spectra (isotopically labeled-minus-unlabeled) obtained for *Rb. sphaeroides* RCs reconstituted with $^{13}C_1$-labeled Q_3 (c) and $^{13}C_4$-labeled Q_3 (d) in the Q_B site. Corresponding double-difference spectra for the Q_A site of *Rb. sphaeroides* RCs (e and f). Arbitrary vertical scale. Data were taken from Breton et al. (*31*, *33*).

calculated for a pure C═O stretching mode (37 cm^{-1}), thus demonstrating some specific coupling between the C═O and C═C modes of Q_B (*33*). Indeed, the pattern and the frequencies of the C═C bands show, for all the RCs, a shift of the positive band at 1610−1614 cm^{-1} to ∼1600 cm^{-1} upon $^{13}C_1$ labeling (Figure 3a−c), and no effect upon $^{13}C_4$ labeling (Figure 3d−f). For isolated Q_3 (Figure 4a,b), the shift of the C═C mode frequency is the same (from 1610 to 1600 cm^{-1}) for both $^{13}C_1$ and $^{13}C_4$ labeling, indicating that the couplings of C═C and C═O modes at the C_1 and C_4 positions are equivalent. It therefore appears that in the Tyr-L209 mutant, as well as in wild-type RCs from *Rb. sphaeroides* and *Rp. viridis*, the coupling of the C═C mode of Q_B with the $^{13}C_1$═O or $^{13}C_4$═O mode is different, indicating that the constraint of the protein at the Q_B site affects the C_1 and C_4 atoms differently. Possible explanations, involving the anchoring of the methyl group at C_5 and/or differences in the conformation of the two methoxy groups at C_2 and C_3, have been discussed in detail in a previous publication (*33*).

IR Fingerprints of Ubiquinone in Vitro and in the Q_A and Q_B Binding Sites of Native RCs. Figure 4 compares the IR fingerprints of the same molecule of ubiquinone (Q_3) in vitro (Figure 4a,b), in the Q_B site (Figure 4c,d), and in the Q_A site (Figure 4e,f) of *Rb. sphaeroides* RCs in the 1720−1520 cm^{-1} range. These spectra show that the IR fingerprint for each isotopomer of ubiquinone is unique and reflects a different conformation of the quinone molecule modulated by its specific interactions with the environment (solvent or protein around Q_A or Q_B). Isolated Q_3 in films shows very comparable isotopic IR patterns for both $^{13}C_1$ and $^{13}C_4$ labeling, with two C═O bands at 1666 and 1647 cm^{-1} shifting to 1620−1621 cm^{-1} and one C═C band at 1610 cm^{-1} shifting to 1600 cm^{-1} (Figure 4a,b). The origin of the splitting of the carbonyl bands in IR spectra of isolated ubiquinones has been previously addressed (*31*, *33*, *46*, *47*, *51*, *52*), and is best explained by the existence of two conformers which differ by the orientation (in the plane or out of the plane of the quinone ring) of the methoxy groups.[4]

Compared to the C═O frequencies at 1650 and 1663 cm^{-1} of ubiquinone in vitro (*31*), the unique band observed at 1640 ± 1 cm^{-1} for the Q_B site (Figure 4c,d) is downshifted by either 10 or 23 cm^{-1}, depending on the conformation of the methoxy groups in the Q_B binding site. On the other hand, the Q_A site of *Rb. sphaeroides* RCs reconstituted with Q_3 displays two bands at 1660 and 1628 cm^{-1} upon $^{13}C_1$ labeling (Figure 4e) and at 1628 and 1601 cm^{-1} upon $^{13}C_4$ labeling (Figure 4f). The large difference in the IR frequency of the two C═O modes of Q_A at 1660 and 1601 cm^{-1} underscores the greatly different interactions of the two carbonyls of Q_A with the protein (*31*, *32*, *35*). In contrast to the dramatic downshift of the frequency of the C_4═O group of Q_A in *Rb. sphaeroides* RCs (49 or 62 cm^{-1}), the 10−23 cm^{-1} frequency downshift observed for both the C_1═O and C_4═O groups of Q_B in native RCs from *Rb. sphaeroides* and *Rp. viridis*, as well as in the Tyr-L209 mutant, is indicative of equivalent hydrogen bonding interactions of the two carbonyls of Q_B with the protein, with a moderate strength of the hydrogen bonds.

Interactions of Q_B with the Protein in Wild-Type RCs and in the Pro-L209 → Tyr Mutant: Comparison of FTIR Data with Crystallographic Structures. In the bacterial RC, the secondary quinone Q_B can exist in at least three principal redox states: the neutral Q_B, the semiquinone Q_B^-, and the quinol Q_BH_2. Among the numerous X-ray structures reported for *Rb. sphaeroides* RCs, only two structures place the secondary quinone in the distal site (*10*, *11*). In the first RC structure describing Q_B in the distal site (*10*), only one carbonyl could form a hydrogen bond to the protein; however, with two possible partners, i.e., the peptide NH group of Ile-L224 and the peptide C═O group of Tyr-L222; this latter interaction would support the view that the ubiquinone in the distal site is present as quinol (*10*). In the structure of RC crystals cooled in the dark at cryogenic temperature (*11*), it was estimated that 95% of the ubiquinone was in the ground-state Q_B, with a major occupation of the distal site (with a single hydrogen bond to Q_B) and a minor population in the proximal site. When Q_B occupied the proximal position in crystals of native RCs, the secondary quinone was presumed to be in the neutral state since no special illumination of the crystals was performed, except in the light-adapted structure of Stowell et al. (*11*) which was estimated to contain 92% $P^+Q_B^-$ charge-separated state. However, the possibility that Q_B is reduced in the crystal prior to or during the collection of X-ray data has not been ruled out as discussed in refs *11* and *22*. Therefore, the redox

[4] When the conformation of the $O-CH_3$ bond is coplanar to the quinone ring, a mesomeric resonance phenomenon induces a frequency downshift of the carbonyl in the meta position (*47*). Since the two methoxy groups cannot simultaneously be in the plane of the ring for steric reasons, the mode composition of each C═O band of isolated ubiquinone arises from equal amounts of the C_1═O mode of one conformer and the C_4═O mode of the other conformer (*31*, *33*, *46*, *47*, *51*). This explains the splitting of the C═O bands for isolated ubiquinone and the observation of similar double-difference spectra for $^{13}C_1$ or $^{13}C_4$ labeling of Q_3 (Figure 4a,b).

state of the quinone in both the distal and proximal sites still presents some ambiguity. It is worth noting that in the various X-ray structures of wild-type (*3*−*9*, *12*) and mutant (*22*, *23*, *28*) RCs where Q_B (neutral or reduced) occupies the proximal binding site, both Q_B carbonyls form polar interactions with the surrounding protein, in contrast to the observation of only one carbonyl interacting with the protein in the distal site (*10*, *11*). In the proximal conformation, one carbonyl of Q_B (or Q_B^-) always accepts a hydrogen bond from the Nδ atom of His-L190, while at the other carbonyl, multiple hydrogen bonds to the protein are described, e.g., to the backbone NH group of Gly-L225 and/or Ile-L224 and/or with the side chain of Ser-L223.

In contrast to crystallographic structures, the FTIR data of native (*33*, *35*) and mutant (*45*) RCs, including the Tyr-L209 mutant (Figure 3c, f), do not indicate heterogeneous bonding of neutral Q_B to the protein. Only one site is detected by IR spectroscopy; i.e., the IR fingerprint of Q_B shows both C═O groups contributing equally to the single 1640 ± 1 cm^{-1} band (Figure 3). Thus, the straightforward interpretation of the FTIR data is that each carbonyl of Q_B is engaged in comparable interactions with the protein at the binding site. Moreover, the highly specific IR fingerprint of the coupling of the C═O and C═C modes measured by the effect of selective labeling of Q_3 at the C_1 or C_4 position is nearly the same for the Q_B sites of all the RCs investigated so far. It can therefore be concluded that the neutral state of the functional Q_B occupies the same binding site in all these RCs. In principle, provided that both carbonyls of Q_B could equivalently interact with the surrounding protein, the interpretation of the FTIR data should not be restricted to either the distal or proximal site. However, in view of the two main distinct sites described in the various X-ray structures of RCs, we herein analyze our data in the frame of neutral Q_B fitting either the proximal or distal Q_B site.

The possibility that the neutral Q_B in wild-type RCs of *Rb. sphaeroides* occupies a distal position cannot be strictly ruled out from the FTIR data. However, this seems to be difficult to reconcile with the available X-ray structural models describing only one hydrogen bond to Q_B in the distal site[5] (*11*, *12*), and in this case, a very specific conformation of the methoxy groups and/or a localized perturbation of the dielectric constant would have to be invoked to compensate for the frequency downshift of the Q_B carbonyl which is not hydrogen bonded to the protein. Furthermore, if neutral Q_B in the wild-type RCs were in the distal conformation, this would be also the case for the Pro-L209 → Tyr mutant, in contrast to the experimental X-ray results on this RC (*28*).

Already for wild-type RCs, the equivalence of frequency of the two carbonyls rather favors the proximal site because of its hydrogen bonding pattern. This fits the proximal Q_B site described for *Rp. viridis* RCs reconstituted with Q_2 (*12*). The FTIR study of the Tyr-L209 mutant RC presented here offers a new way to discriminate between the two possibilities in wild-type *Rb. sphaeroides* RCs. Only one site has been described for the location of the secondary quinone in the dark-adapted structure at 5 °C of the crystals of the Tyr-L209 mutant (*28*). This site is the proximal one. Since the vibrational properties of the neutral secondary quinone in the Tyr-L209 mutant are essentially the same as those described in native RCs (Figure 3), it therefore appears that the FTIR data on native RCs fit the Q_B interactions described in the proximal conformation better than those reported for the distal Q_B site. Consequently, we strongly favor the proximal Q_B conformation as the dominant binding site of neutral Q_B in native functional RCs from *Rb. sphaeroides* and *Rp. viridis*. This is in contrast with the distal Q_B structure found in dark-adapted crystals of *Rb. sphaeroides* RCs (*11*).

These FTIR data strengthen the view that the proximal site is the active site for electron transfer to Q_B in native functional RCs. Very recently, it has been suggested that the Q_B movement is unlikely to be the dominant contribution to the conformational gate that controls the first electron transfer to Q_B in native RCs. Notably, the rate of electron transfer from Q_A^- to Q_B in *Rb. sphaeroides* RCs has been found to be independent of the isoprene chain length of Q_B (*27*, *53*, *54*). In agreement with these spectroscopic measurements, earlier FTIR studies of native RCs from *Rb. sphaeroides* have shown that the IR fingerprint of Q_B does not change upon varying the isoprene chain length (from one unit to three, six, eight, and ten units) of the ubiquinone (*33*, *34*). These FTIR results therefore do not indicate an influence of the tail length on the interactions of Q_B with the protein, and thus on its position within the RC. Moreover, the absence of a significant change in the first electron transfer rate in the Tyr-L209 mutant relative to that of native RCs is not consistent with the movement of Q_B representing the rate-limiting step (*26*, *27*). Other sources of protein conformational change and/or protonation change of carboxylic acids (*55*, *56*), such as the observed protonation of Glu-L212 coupled with electron transfer from Q_A^- to Q_B (*38*, *39*, *57*), might contribute to the gating mechanism.

ACKNOWLEDGMENT

We thank J. Thomas Beatty for careful reading of the manuscript.

REFERENCES

1. Okamura, M. Y., Paddock, M. L., Graige, M. S., and Feher, G. (2000) *Biochim. Biophys. Acta 1458*, 148−163.
2. Fritzsch, G., and Kuglstatter, A. (1999) in *The Photochemistry of Carotenoids* (Frank, H. A., Young, A. J., Britton, G., and Cogdell, R. J., Eds.) pp 99−122, Kluwer Academic Publishers, Dordrecht, The Netherlands.
3. Allen, J. P., Feher, G., Yeates, T. O., Komiya, H., and Rees, D. C. (1988) *Proc. Natl. Acad. Sci. U.S.A. 85*, 8487−8491.
4. El-Kabbani, O., Chang, C.-H., Tiede, D., Norris, J., and Schiffer, M. (1991) *Biochemistry 30*, 5361−5369.
5. Chirino, A. J., Lous, E. J., Huber, M., Allen, J. P., Schenck, C. C., Paddock, M. L., Feher, G., and Rees, D. C. (1994) *Biochemistry 33*, 4584−4593.
6. Arnoux, B., and Reiss-Husson, F. (1996) *Eur. Biophys. J. 24*, 233−242.
7. Deisenhofer, J., and Michel, H. (1989) *EMBO J. 8*, 2149−2170.
8. Deisenhofer, J., Epp, O., Sinning, I., and Michel, H. (1995) *J. Mol. Biol. 246*, 429−457.
9. Lancaster, C. R. D., Ermler, U., and Michel, H. (1995) in *Anoxygenic Photosynthetic Bacteria* (Blankenship, R. E., Madigan, M. T., and Bauer, C. E., Eds.) pp 503−526, Kluwer Academic Publishers, Dordrecht, The Netherlands.
10. Ermler, U., Fritzsch, G., Buchanan, S. K., and Michel, H. (1994) *Structure 2*, 925−936.

[5] One reviewer has suggested that Q_B in the distal site might be moderately hydrogen bonded to the backbone at Ile-L224 and to a water molecule that was not resolved in the X-ray structure. In such a case, the FTIR data would not be incompatible with the binding of Q_B in the distal site.

11. Stowell, M. H. B., McPhillips, T. M., Rees, D. C., Soltis, S. M., Abresch, E., and Feher, G. (1997) *Science 276*, 812−816.
12. Lancaster, C. R. D., and Michel, H. (1997) *Structure 5*, 1339−1359.
13. Lancaster, C. R. D. (1998) *Biochim. Biophys. Acta 1365*, 143−150.
14. Zachariae, U., and Lancaster, C. R. D. (2001) *Biochim. Biophys. Acta 1505*, 280−290.
15. Graige, M. S., Feher, G., and Okamura, M. Y. (1998) *Proc. Natl. Acad. Sci. U.S.A. 95*, 11679−11684.
16. Rabenstein, B., Ullmann, G. M., and Knapp, E.-W. (2000) *Biochemistry 39*, 10487−10496.
17. Grafton, A. K., and Wheeler, R. A. (1999) *J. Phys. Chem. B 103*, 5380−5387.
18. Alexov, E. G., and Gunner, M. R. (1999) *Biochemistry 38*, 8253−8270.
19. Cherepanov, D. A., Bibikov, S. I., Bibikova, M. V., Bloch, D. A., Drachev, L. A., Gopta, O. A., Oesterhelt, D., Semenov, A. Y., and Mulkidjanian, A. Y. (2000) *Biochim. Biophys. Acta 1459*, 10−34.
20. Walden, S. E., and Wheeler, R. A. (2002) *J. Phys. Chem. B 106*, 3001−3006.
21. Ridge, J. P., van Brederode, M. E., Goodwin, M. G., van Grondelle, R., and Jones, M. R. (1999) *Photosynth. Res. 59*, 9−26.
22. McAuley, K. E., Fyfe, P. K., Ridge, J. P., Cogdell, R. J., Isaacs, N. W., and Jones, M. R. (2000) *Biochemistry 39*, 15032−15043.
23. Pokkuluri, P. R., Laible, P. D., Deng, Y.-L., Wong, T. N., Hanson, D. K., and Schiffer, M. (2002) *Biochemistry 41*, 5998−6007.
24. Hanson, D. K., Baciou, L., Tiede, D. M., Nance, S. L., Schiffer, M., and Sebban, P. (1992) *Biochim. Biophys. Acta 1102*, 260−265.
25. Baciou, L., and Michel, L. (1995) *Biochemistry 34*, 7967−7972.
26. Tandori, J., Sebban, P., Michel, H., and Baciou, L. (1999) *Biochemistry 38*, 13179−13187.
27. Xu, Q., Baciou, L., Sebban, P., and Gunner, M. R. (2002) *Biochemistry 41*, 10021−10025.
28. Kuglstatter, A., Ermler, U., Michel, H., Baciou, L., and Fritzsch, G. (2001) *Biochemistry 40*, 4253−4260.
29. Breton, J., Thibodeau, D. L., Berthomieu, C., Mäntele, W., Verméglio, A., and Nabedryk, E. (1991) *FEBS Lett. 278*, 257−260.
30. Breton, J., Berthomieu, C., Thibodeau, D. L., and Nabedryk, E. (1991) *FEBS Lett. 288*, 109−113.
31. Breton, J., Boullais, C., Burie, J.-R., Nabedryk, E., and Mioskowski, C. (1994) *Biochemistry 33*, 14378−14386.
32. Brudler, R., de Groot, H. J. M., van Liemt, W. B. S., Steggerda, W. F., Esmeijer, R., Gast, P., Hoff, A. J., Lugtenburg, J., and Gerwert, K. (1994) *EMBO J. 13*, 5523−5530.
33. Breton, J., Boullais, C., Berger, G., Mioskowski, C., and Nabedryk, E. (1995) *Biochemistry 34*, 11606−11616.
34. Brudler, R., de Groot, H. J. M., van Liemt, W. B. S., Gast, P., Hoff, A. J., Lugtenburg, J., and Gerwert, K. (1995) *FEBS Lett. 370*, 88−92.
35. Breton, J., and Nabedryk, E. (1996) *Biochim. Biophys. Acta 1275*, 84−90.
36. Breton, J. (1997) *Proc. Natl. Acad. Sci. U.S.A. 94*, 11318−11323.
37. Hucke, O., Schmid, R., and Labahn, A. (2002) *Eur. J. Biochem. 269*, 1096−1108.
38. Nabedryk, E., Breton, J., Hienerwadel, R., Fogel, C., Mäntele, W., Paddock, M. L., and Okamura, M. Y. (1995) *Biochemistry 34*, 14722−14732.
39. Hienerwadel, R., Grzybek, S., Fogel, C., Kreutz, W., Okamura, M. Y., Paddock, M. L., Breton, J., Nabedryk, E., and Mäntele, W. (1995) *Biochemistry 34*, 2832−2843.
40. Nabedryk, E., Breton, J., Okamura, M. Y., and Paddock, M. L. (1998) *Biochemistry 37*, 14457−14462.
41. Nabedryk, E., Breton, J., Joshi, H. M., and Hanson, D. K. (2000) *Biochemistry 39*, 14654−14663.
42. Nabedryk, E., Breton, J., Okamura, M. Y., and Paddock, M. L. (2001) *Biochemistry 40*, 13826−13832.
43. Breton, J., Nabedryk, E., Allen, J. P., and Williams, J. C. (1997) *Biochemistry 36*, 4515−4525.
44. Breton, J., Bibikova, M., Oesterhelt, D., and Nabedryk, E. (1999) *Biochemistry 38*, 11541−11552.
45. Breton, J., Nabedryk, E., Boullais, C., Mioskowski, C., Paddock, M. L., Feher, G., and Okamura, M. Y. (1997) *Biophys. J. 72*, A7.
46. Burie, J.-R., Boullais, C., Nonella, M., Mioskowski, C., Nabedryk, E., and Breton, J. (1997) *J. Phys. Chem. B 101*, 6607−6617.
47. Boullais, C., Nabedryk, E., Burie, J.-R., Nonella, M., Mioskowski, C., and Breton, J. (1998) *Photosynth. Res. 55*, 247−252.
48. Verméglio, A. (1977) *Biochim. Biophys. Acta 459*, 516−524.
49. Wraight, C. A. (1977) *Biochim. Biophys. Acta 459*, 525−531.
50. Axelrod, H. L., Abresch, E. C., Paddock, M. L., Okamura, M. Y., and Feher, G. (2000) *Proc. Natl. Acad. Sci. U.S.A. 97*, 1542−1547.
51. Nonella, M., and Brändli, C. (1996) *J. Phys. Chem. 100*, 14549−14559.
52. Robinson, H. H., and Khan, S. D. (1990) *J. Am. Chem. Soc. 112*, 4728−4731.
53. Li, J., Takahashi, E., and Gunner, M. R. (2000) *Biochemistry 39*, 7445−7454.
54. McComb, J. C., Stein, R. R., and Wraight, C. A. (1990) *Biochim. Biophys. Acta 1015*, 156−171.
55. Li, J., Gilroy, D., Tiede, D. M., and Gunner, M. R. (1998) *Biochemistry 37*, 2818−2829.
56. Xu, Q., and Gunner, M. R. (2002) *Biochemistry 41*, 2694−2701.
57. Mezzetti, A., Nabedryk, E., Breton, J., Okamura, M. Y., Paddock, M. L., Giacometti, G., and Leibl, W. (2002) *Biochim. Biophys. Acta 1553*, 320−330.
58. Spiedel, D., Roszak, A. W., McKendrick, K., McAuley, K. E., Fyfe, P. K., Nabedryk, E., Breton, J., Robert, B., Cogdell, R. J., Isaacs, N. W., and Jones, M. R. (2002) *Biochim. Biophys. Acta 1554*, 75−93.

BI026565K